Journal of Chromatography B 1182 (2021) 122925

Contents lists available at ScienceDirect

Journal of Chromatography B

journal homepage: www.elsevier.com/locate/jchromb

nES-DMA with Charge-reduction based on Soft X-ray Radiation: Analysis of a Recombinant Monoclonal Antibody

Nicole Y. Engel, Nicole Puffler, Martina Marchetti-Deschmann, Günter Allmaier, Victor U. Weiss *

Institute of Chemical Technologies and Analytics, TU Wien (Vienna University of Technology), Vienna, Austria

ARTICLE INFO

Keywords:
Differential mobility analysis
Gas-phase electrophoresis
nES GEMMA
Recombinant monoclonal antibody
IdeS

ABSTRACT

Due to the fast growing importance of monoclonal antibodies in biomedical research, bioanalytics and human therapy, sensitive, fast and reliable methods are needed to monitor their production, target their characteristics, and for their final quality control. Application of a nano electrospray (nES) with soft X-ray radiation (SXR) based charge reduction and differential mobility analysis (DMA, aka nano electrospray gas-phase electrophoretic mobility molecular analysis, nES GEMMA) allows the size-separation and detection of macromolecules and (bio-) nanoparticles from a few nm up to several hundreds of nm in diameter in a native-like environment. The current study focuses on the analysis of a 148 kDa recombinant monoclonal antibody (rmAb) with the above mentioned instrumental setup and applying an universal detector, i.e. a water-based condensation particle detector (CPC). Next to the intact rmAb, its aggregates and fragment products after digestion with IdeS protease were analyzed. Additionally, influence of temperature treatment and pH variation on the stability of the rmAb was monitored. In this context, changes in electrophoretic mobility diameter (EMD) values, peak shape, and signal intensity based on particle numbers were of interest. Molecular weights calculated by application of a correlation derived from respective standard protein compounds were compared to mass spectrometric values and were found to be in good accordance. To conclude, we demonstrate that nES-DMA is a valuable tool in the characterization and quality control of rmABs.

1. Introduction

Recombinant monoclonal antibodies (rmAb) have become major therapeutic and diagnostic agents applied for treatment and detection of many diseases like cancer, inflammation or infectious diseases. Currently, rmAbs are for instance under investigation as an early intervention against COVID-19 [1]. Thus, it is of importance to find suitable methods to monitor their production processes and product quality with focus on intact molecules, the formation of specific and unspecific aggregates and degradation products. Typical analytical methods focusing on separation of analytes according to their size are size exclusion chromatography (SEC), capillary gel electrophoresis, mass spectrometry or similar. Alternatively, we are concentrating on nES-DMA (this setup is also called nES GEMMA, LiquiScan-ES, macro ion mobility spectrometer (macroIMS) or scanning mobility particle sizer (SMPS) in literature) for rmAb analysis. This method is working at atmospheric pressure under relatively mild conditions, preserving analytes in a not easily targetable size and MW range in their native state. Even fragile, non-covalent interactions are kept intact as demonstrated for instance for complexes between antibody fragments and a virus-like particle [2] or between glycoproteins and lectins [3]. Hence nES-DMA offers an ideal basis for monitoring rmAbs, their specific aggregates and forced (e.g. by enzymes) or unforced degradation products. The system separates single-charged, surface-dry analytes in the gas-phase according to their electrophoretic mobility diameters (EMDs), which can be directly correlated to particle diameters in case of spherical analytes [4–6].

In general, EMD determination of analytes is highly repeatable. In

Abbreviations: ACN, acetonitrile; NH_4OAc, ammonium acetate; CPC, condensation particle counter; EMD, electrophoretic mobility diameter; GEMMA, gas-phase electrophoretic mobility molecular analysis; HPLC, high performance liquid chromatography; MALDI, matrix-assisted laser desorption/ionization; MS, mass spectrometry; nDMA, nano differential mobility analyzer; nES, nano electrospray; rmAb, recombinant monoclonal antibody; SA, sinapinic acid; SXR, soft X-ray radiation; TFA, trifluoroacetic acid.

* Corresponding author at: Institute of Chemical Technologies and Analytics, TU Wien, Getreidemarkt 9/164-IAC, 1060 Vienna, Austria.
E-mail address: victor.weiss@tuwien.ac.at (V.U. Weiss).

https://doi.org/10.1016/j.jchromb.2021.122925
Received 5 February 2021; Received in revised form 5 August 2021; Accepted 1 September 2021
Available online 8 September 2021

case analyte quantification should be based on nES-DMA measurements as well, daily instrument calibration and tight control of gas and liquid flow rates is necessary [7]. Up to date, the approach of differential mobility analysis of single-positive or negative charged analytes has been explored for a wide array of biomedical applications [8–15]. The system combines a nano electrospray (nES) unit for transferring analytes from the liquid to the gas-phase, a nano differential mobility analyzer (nDMA) for size-separation, and an ultrafine condensation particle counter (CPC) for single particle detection. During analysis, analytes dissolved in a volatile electrolyte are electrosprayed from a fused silica capillary in the nES unit. In order to generate a stable electrospray, the nES unit is operated in cone-jet mode by variation of the electric field applied to the tip of the capillary. Consequently, multiple-charged droplets are released from the Taylor cone [16–18]. Supported by a sheath gas flow of dried and particle-free air and CO_2, the multiple-charged droplets are concomitantly dried and charge equilibrated as they are carried through a bipolar atmosphere induced by a low energy soft X-ray radiation (SXR) discharger (<9.5 keV). Mainly neutral, polydisperse nanoparticles, as well as a small amount of single (<5 % for particles below 10 nm EMD), and a negligible amount of multiple charged particles are obtained [19–22].

After charge equilibration, particles are directed into the cylindrical nDMA. By application of a tunable negative voltage to the center electrode of the nDMA in combination with an orthogonal laminar high-speed flow of sheath air, the analytes are separated according to their EMD. Only positively charged particles are attracted towards the inner electrode, whereas negatively charged particles are repelled, and neutral particles leave the nDMA unaffected. At a certain applied voltage, positively charged analytes of a particular EMD can leave the nDMA towards the universal detector (CPC). The possibility to adjust the voltage enables the scanning of a certain size range.

Subsequently, the monodisperse (monomobile) particles are guided after gas-phase electrophoretic separation through the continuous-flow CPC, in which they are enlarged by condensation of supersaturated water vapor [23,24]. These single droplets can finally be detected by laser light scattering resulting in a particle number-based concentration as recommended by the European Commission for nanoparticle characterization (2011/696/EU from October 18th, 2011). Plotting EMDs against particle counts per volume yields a corresponding spectrum. Finally, the molecular weight (MW) of an analyte can be calculated by applying an EMD/MW correlation derived from standards of the appropriate compound class, i.e. proteins [25].

In the course of this study a formulated rmAb was analyzed with the described instrumental setup. The ability to separate and detect rmAbs, aggregates thereof as well as fragment products after digestion with IdeS was investigated. Moreover, the rmAb was exposed to varying pH values and temperatures and its behavior under stress-conditions was monitored with the device. Next to that, the repeatability and accuracy of rmAb measurements were investigated with special focus on size determination and quantitation. Results were compared to values obtained with matrix-assisted laser desorption/ionization (MALDI) mass spectrometry (MS).

2. Materials and methods

2.1. Materials

NH_4OAc (Cat. No. 431311), trifluoroacetic acid (TFA, Cat. No. 302031), sinapic acid (SA, Cat. No. D7927), ammonium hydroxide (Cat. No. 221228), and acetic acid (Cat. No. 33209) were obtained from Sigma-Aldrich. Acetonitrile (ACN, Cat. No. 100030) was purchased from Merck.

For all solutions, water of Millipore grade (18.2 MΩcm resistivity at 25 °C) from a Simplicity UV water purification system (Millipore, Molsheim, France) was used. Prior to application, all electrolytes were filtered with 0.2 μm pore size syringe filters (sterile, surfactant-free cellulose acetate membrane; Sartorius, Cat. No. 16534-K).

2.2. Sample preparation

A rmAB of therapeutic grade was dissolved in 5 mM histidine and 60 mM trehalose buffer (pH 6.0). For exchange to 40 mM NH_4OAc (pH 8.0, 7.4 or 5.0 adjusted with acetic acid or ammonium hydroxide, respectively) and sample concentration 10 kDa centrifugal filters (polyethersulfone membrane; VWR, Cat. No. 516–0229) were used according to the manufacturer's protocol. The rmAB was then diluted to the required concentrations ranging from 4.7 to 7527.0 nM.

2.3. Sub-unit fragmentation of rmAb with IdeS protease

For digestion of the rmAb to $F(ab')_2$ and Fc fragments, FragIT MicroSpin Columns (Genovis, Cat. No. A0-FR6-010) containing IdeS enzyme from *Streptococcus pyogenes* covalently coupled to agarose beads were used according to manufacturer's protocol. 5 mg/mL rmAb in 40 mM NH_4OAc (pH 7.4) were applied to the column and incubated for 15 min at room temperature by end-over-end mixing. Additionally, the column was incubated overnight at 22 °C and 600 rpm. The resulting antibody sample was further diluted with 40 mM NH_4OAc (pH 7.4) for subsequent measurements.

2.4. Nano-DMA with SXR analysis

A system (from TSI Inc, Shoreview, MN, USA) was put together consisting of a nano electrospray aerosol generator including a soft x-ray source (model 3482), a DMA (model 3085A), and a nano water-based CPC (model 3788). Samples were delivered by direct infusion via a syringe pump (NE-1000, New Era Pump Systems, Farmingdale, NY, USA) at a flow rate of 6 μL/min. nES sheath gas (CO_2 and filtered, dried air from a membrane dryer Superplus; Ludvik Industriegeräte, Vienna, Austria) was set to 1.37 L per minute (Lpm) and voltages were adjusted for stable cone jet mode (1.39–1.45 kV). nDMA laminar flow was set to 30 L per minute with scan times of 11 or 56 s (3 s retrace and 1 s lag time each in order to set the voltage to initial conditions). Scans from 2 to 45 nm EMD were acquired during 20 min of continuous sampling. All data result from triplicate measurements and were interpreted with the OriginPro software (v 9.1.0, OriginLab).

2.5. MALDI-MS

Experiments were performed on the MALDI-TOF-MS AXIMA TOF^2 (Shimadzu Kratos Analytical, Manchester, UK) equipped with a nitrogen laser ($\lambda = 337$ nm) and operated in linear positive ion mode. Samples were prepared on stainless steel MALDI target plate using the dried-droplet technique. Before drying at room temperature, samples were applied 1:1 (v:v) with 10 mg/mL SA in 0.1% TFA/ACN (1:1, v:v) as MALDI-MS matrix to a final amount on target of 2, 4, and 8 pmol for the pure rmAb and 2.8 and 5.6 pmol for the IdeS digestion.

3. Results

A schematic drawing of the nES-DMA system applied in rmAb analysis is depicted in Fig. 1. The sample can be introduced either by direct infusion via a syringe pump as in the current case at a low μL/min flow or, alternatively, by *on-line* coupling the nES-DMA system with a liquid chromatography system. In the latter case a low mL/min flow high performance liquid chromatography (HPLC) system is possible [26]. In order to adjust the flow rate created by the syringe pump (5 – 10 μL/min) to a suitable one for the capillary (50 – 100 nL/min) a flow splitter (T-piece) is used. In the nES source the analytes are electrosprayed through a cone-tipped fused silica capillary (Fig. 1A). In contrast to older devices including a radioactive Po-210 source, the generated multiply charged droplets in next generation devices

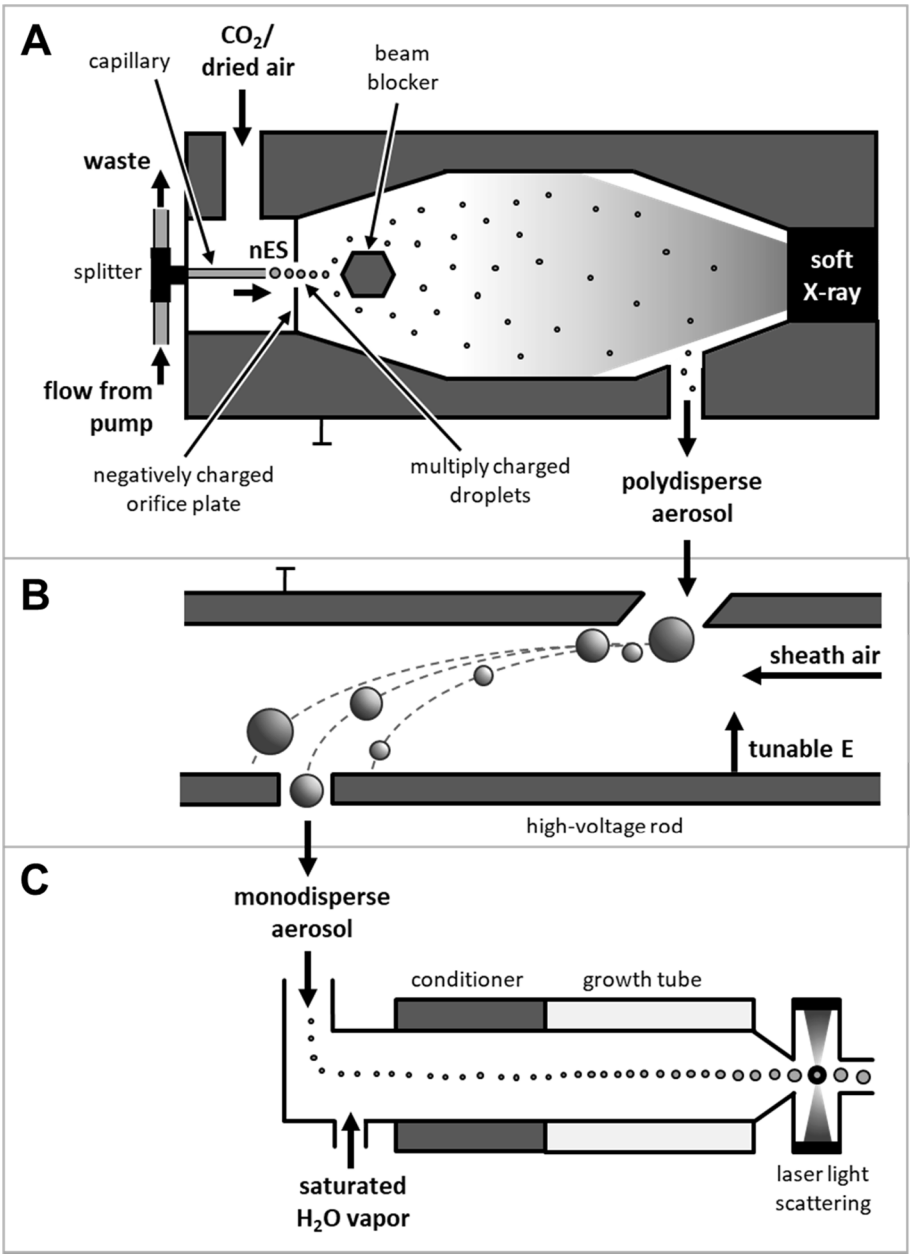

Fig. 1. Schematic representation of the nES-DMA including the SXR device. Analytes are electrosprayed, dried, and charge reduced to polydisperse aerosol in the nES unit (A). Single positive charged, dry particles are then separated according to their EMD in the DMA (B) and detected in the water-driven CPC (C).

subsequently pass a bipolar atmosphere generated by soft X-ray radiation, that can be simply turned on and off. There, particles are dried and charge equilibrated. A beam blocker protects the Taylor cone formed at the capillary tip from the direct impact of the X-ray radiation. In the nDMA, the single-positive charged, polydisperse particles are then separated according to their surface-dry size (EMD) by application of an electric field perpendicular to a sheath flow of compressed air (Fig. 1B). The obtained monodisperse particle fractions are finally detected with a water-driven CPC via an optical system (laser light scattering, Fig. 1C).

3.1. Size determination (EMD) of intact rmAb

For determining the EMD, the rmAb was transferred into a volatile electrolyte of 40 mM ammonium acetate (NH_4OAc, pH 8.0) and diluted to the intended concentrations. Fig. 2 exemplarily displays the size spectra of a lower concentrated 470.4 nM rmAb solution in comparison to a high concentration of 5645.3 nM. Both spectra show a dominating peak of single charged species $[rmAb]^+$ representing the monomer of the rmAb with an EMD of 9.46 ± 0.13 nm. Additionally, the rmAb dimer with an EMD of 11.63 ± 0.10 nm can be observed in both cases. For the higher concentrated analyte also EMD values for the trimer (EMD: 13.22 ± 0.15 nm) and tetramer (EMD: 14.34 ± 0.09 nm) can be determined. In addition, peaks for penta- and hexamers are visually distinguishable. In contrast to the lower concentrated rmAB solution the overall ratio of multimers in regard to the monomer is much higher resulting from the nES process: In case the number of analytes exceeds the number of nanodroplets, statistically more than one particle can be found per droplet. Subsequently, these analytes cluster and are detected as corresponding multimers.

It is of note that these nES induced aggregates are hardly differentiable from biospecific ones. Slight differences can, however, be found upon *on-line* hyphenation of a SEC setup and a nES-DMA system, relating biospecific protein aggregates in the liquid phase to corresponding aggregates detected in the gas-phase and not to nES induced ones [26].

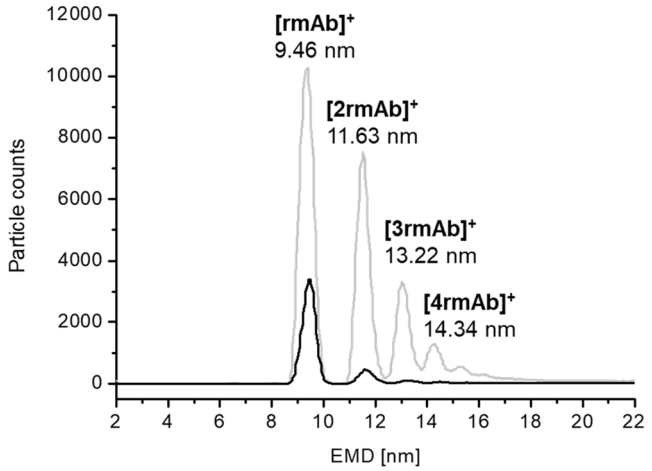

Fig. 2. Nano ES-DMA/SXR analysis of different concentrations of the rmAb: 470.4 nM (black) and 5645.3 nM (grey).

Alternatively, nES-DMA measurements at different analyte concentrations yields a constant ratio of multimers in regards to the monomers only in the absence of spray-induced aggregation (see Supplementary Figure SF1 for exemplary spectra). Hence, by variation of the analyte concentration in samples, nES induced analyte aggregation can be excluded.

Using protein standards of known MWs, an EMD/MW correlation can be established ($y = ax^b$, with $a = 0.3920$ and $b = 2.6388$; for details refer to supporting information, Supplementary Figure SF2 and Supplementary Table ST1). Thus the MW of the rmAb monomer can be derived leading to a value of 147.4 ± 5.3 kDa. This MW is in very good accordance to MALDI MS analyses of the identical rmAb preparation resulting in 148.0 ± 0.7 kDa.

3.2. Analysis of rmAb digested with IdeS protease

Next to the pure antibody solution, rmAb was also treated with IdeS protease. For better digestion conditions, the rmAb was transferred to 40 mM NH_4OAc with a pH of 7.4. Subsequently, the solution was applied to a microspin column containing the enzyme. For a higher turnover rate, the incubation time was prolonged and the rmAb was kept shaking overnight in the column. Fig. 3 compares the rmAb before and after enzymatically triggerd fragment formation. About 86 % of the intact rmAb was cleaved after the digestion. Next to remaining intact rmAb (9.45 ± 0.03 nm), signals at 6.49 ± 0.03 nm and 8.32 ± 0.03 nm can be observed corresponding to the Fc and $F(ab')_2$ fragments, respectively. Application of the established EMD/MW correlation yielded MW values of 54.5 ± 0.6 kDa for the Fc fragment and 105.0 ± 1.2 kDa for the $F(ab')_2$ fragment. Again, these were in good agreement with MALDI linear time-of-flight MS derived values of 48.1 ± 0.1 and 97.4 ± 0.2 kDa. However, a slightly higher deviation of nES-DMA derived results from MS data than for intact rmAbs probably results from the applied EMD/MW correlation focusing on the size and MW range of intact rmAbs and corresponding aggregates. Application of further standards in the lower EMD range will significantly increase the fit between nES-DMA and MS derived data also for Fc and $F(ab')_2$ fragments.

3.3. Concentration dependence of the rmAb signal

The concentration dependent multimer formation during nES-DMA analysis of the rmAb as well as influences on the signal in regard to height/area, peak width (FWHM), and EMD were further investigated. Fig. 4 displays a dilution experiment for the rmAB covering a concentration range from 4.7 to 7527.0 nM. Inter-day and intra-day variability was checked for measurements in a set of three repetitions. The corresponding peak characteristics for the monomeric, dimeric, and trimeric rmAB signals were plotted against the rmAB concentration.

Especially the determination of the EMD showed a good repeatability with only low variations. Inter-day variations of the monomeric peak EMD was below 1.4 % RSD for each concentration and 0.9 % on an average over the whole concentration range. Dimeric and trimeric peaks showed comparably low deviations (inter-day: 0.9 and 1.1 % RSD, respectively). Intra-day deviations resulted in values below 0.02 % RSD for monomeric and dimeric peaks and 0.2 % RSD for trimeric peaks.

Low standard deviations were also observed for monomeric peak widths (FWHM) having an average value of 0.59 ± 0.02 nm: below 5.3 % RSD for each concentration and below 4.1 % RSD on average for the whole concentration range with the exception of two higher values at the lowest concentrations (0.72 ± 0.03 nm for 4.7 nM and 0.63 ± 0.02 nm for 18.8 nM). FWHMs of rmAb dimers (0.63 ± 0.05 nm) and trimers (0.72 ± 0.11 nm) showed greater deviations of 7.3 % RSD and 15.4 % RSD, respectively. In both cases, FWHM values were slowly decreasing with increasing concentrations.

Intra-day variations for peak height and area were rather low with an average value of 4.4 % RSD, however inter-day measurements showed deviations increasing up to 26 % RSD for the monomer and even higher for dimers and trimers.

In Fig. 5, the rmAB concentrations were plotted against the corresponding peak areas for the monomeric and dimeric rmAB signals. As expected, signal intensity increased with higher concentrations.

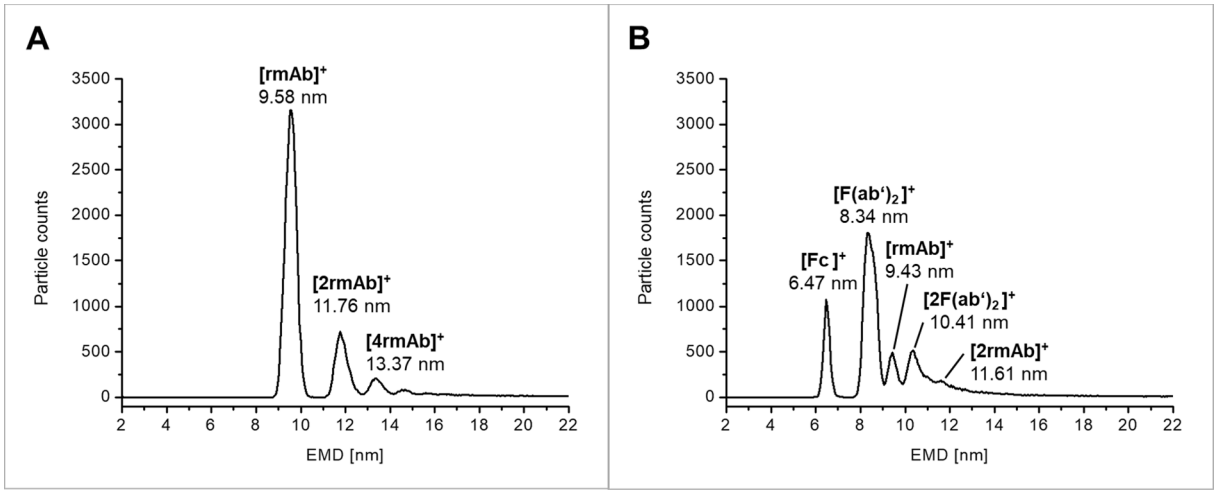

Fig. 3. Nano ES-DMA/SXR analysis of intact rmAb (A) and rmAb digested with IdeS protease (B).

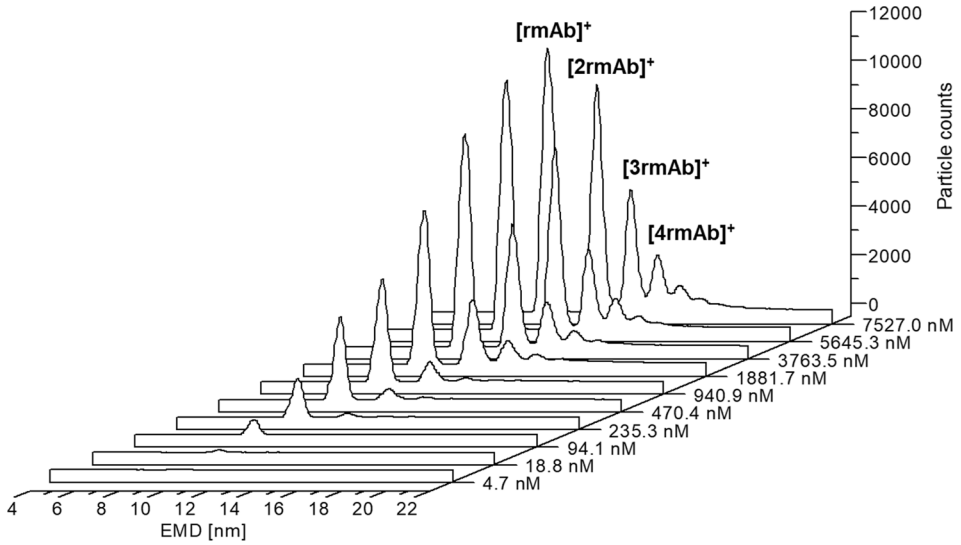

Fig. 4. Nano ES-DMA/SXR spectra of a dilution series of rmAb ranging from 4.7 to 7527.0 nM.

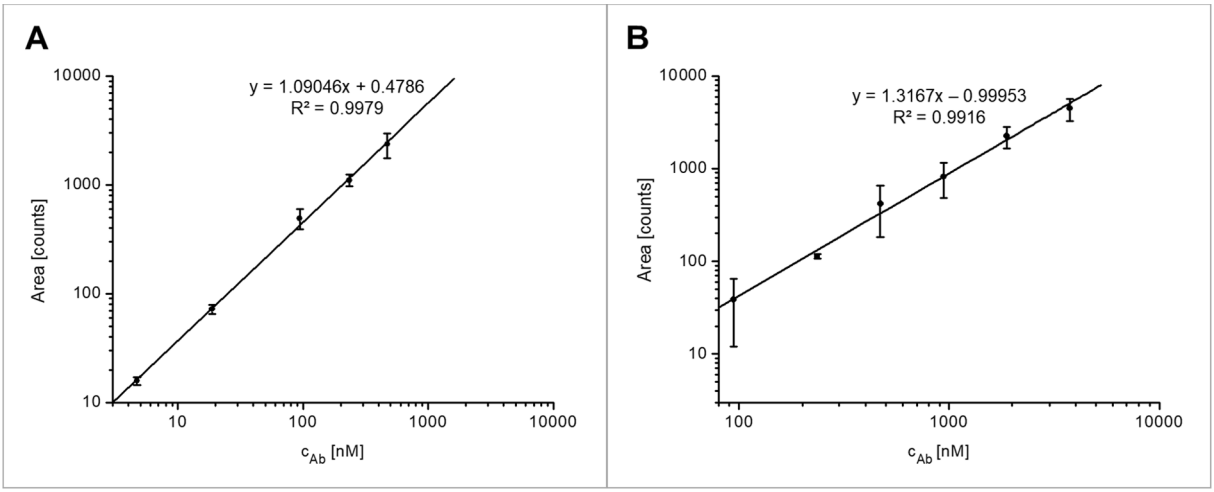

Fig. 5. Linear plot of rmAb concentrations against corresponding peak areas of the monomeric form of rmAb (A) and the dimeric form of rmAb (B).

However, the calibration was not linear for the full concentration range. The measured upper limit of the linear range for the antibody monomer was approx. 500 nM (Fig. 5A). At higher concentrations the amount of multimers formed during the nES process increases and thus influences the linearity of the measured monomer concentration. The measured dimers (Fig. 5B) and trimers (data not shown), however, showed increased linearity, yet of lesser sensitivity (slope of linear regression).

In order to define LOD and LOQ of the analysis, pure background electrolyte (40 mM NH_4OAc, pH 8.0) was analyzed and its mean value in the range of 9 to 11 nm as well as the regarding SD calculated. The LOD was then determined as the mean value plus three times SD, the LOQ as the mean value plus 10 times SD, which resulted in a LOD and LOQ of 5 and 10 nM, respectively. These values were in good accordance with the measurements of 4.7 and 18.8 nM having a signal to noise ratio over 5 and 20, respectively.

3.4. Influence of scan time, as well as pH and temperature treatment of rmAb

Besides analyzing rmAb dilutions and digestion products, the antibody was also measured after temperature treatment and at a lower pH of 5.0. Additionally, we also investigated a reduction of the scan time from 56 s to 11 s per scan while keeping the over-all measurement time constant at 20 min. With this latter change in setup, we intended to study, if sample analysis can be accelerated in order to generate a higher analyte throughput.

The change of the pH from 8.0 to 5.0 at a concentration of 235.3 nM did not affect the determined EMDs (monomer: 9.46 ± 0.01 nm, dimer: 11.71 ± 0.01, trimer: 13.32 ± 0.03 nm, Fig. 6A). However, peak widths, heights, and areas were elevated for all observable peaks. For instance, the monomer width and height were about 10 % increased, its area about 19 %. Dimer and trimer showed even higher deviations.

In contrast to that, reducing the scan speed to 11 s had a major overall impact on the rmAb signal (Fig. 6B). The obtained EMDs of the rmAb were detected at significantly higher values: the monomer was found at 9.90 ± 0.05 nm, the dimer at 12.21 ± 0.05 nm, and the trimer at 13.79 ± 0.11 nm. Moreover, much lower monomer signal intensity values were observed with an average about 24 % smaller peak areas, 46 % decreased heights, and 41 % broader peaks. Again, dimers and trimers were influenced more severely. Additionally, the linear range was increased having a measured upper limit of approx. 3800 nM for the monomer. In all cases, deviations and repeatability was comparable to or even better than measurements with 56 s.

Next to that, the influence of temperature treatment of rmAB samples

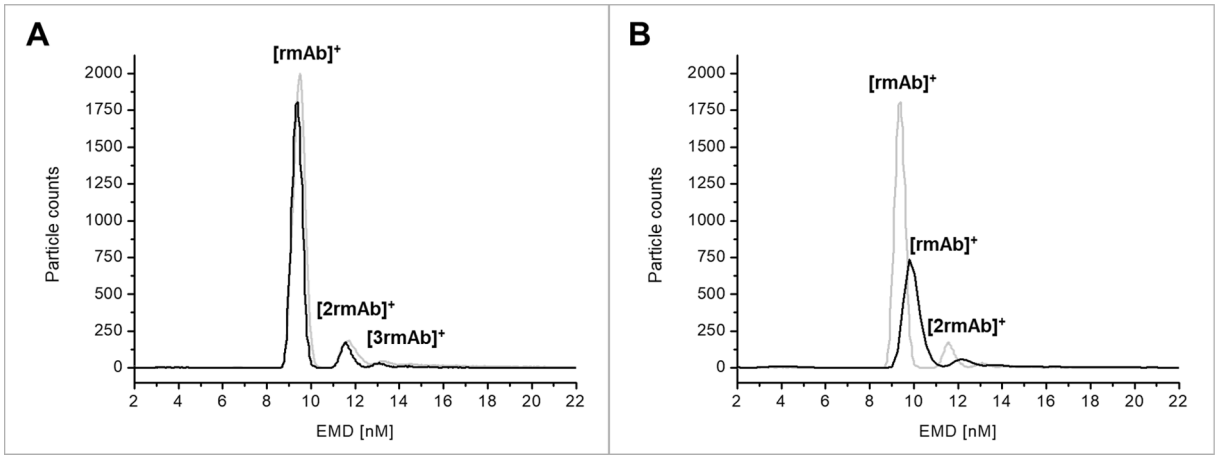

Fig. 6. (A) Nano ES-DMA/SXR spectra of rmAb in 40 mM NH_4OAc at pH 8.0 (black) and pH 5.0 (grey). (B) Nano ES-DMA/SXR spectra of rmAb in 40 mM NH_4OAc measured with a scan time of 11 s (black) and 56 s (grey).

prior to analysis was studied (Fig. 7). Incubation of the sample for 15 min at temperatures from RT up to 70 °C directly before measurement did not seem to influence the stability of this specific rmAb. Above this temperature, i.e. incubation at 75 °C and 80 °C and the indicated heating times, a drastic decrease in rmAb derived signals was observed.

4. Discussion

nES-DMA with SXR is a versatile tool for straightforward and fast size-analysis of antibodies. Moreover, it proved the ability to separate and detect rmAb monomers simultaneously together with non-covalent multimers as well as enzyme-generated large rmAb fragments. Observed EMD values and corresponding calculated MWs based on an EMD/MW correlation were in good agreement to MALDI MS derived MWs.

Investigating the occurrence of rmAb aggregates requires working with low concentrations. As shown in the nES-DMA experiments with higher antibody concentrations, the ratio of detected multimers increased with rmAb concentration. These multimers are nonspecific and formed in gas-phase during the nES process. The higher analyte amount statistically increases the chance of the occurrence of two or three analytes in one droplet [6,23,27]. After evaporation they can be observed as artificial unspecific oligomers. This instance also limits the linear range of rmAb monomers as they are increasingly detected as oligomers at higher concentrations. For distinguishing biospecific oligomers from nonspecific ones, the rmAB concentration is reduced resulting in the disappearance of nonspecific oligomers, At the same time specific rmAb oligomers are preserved. In addition, working with low concentrations advantageously diminishes overall sample consumption.

Next to the analysis of rmAb monomers and aggregates, also antibody fragments can be clearly separated and detected by this device. The enzyme IdeS fragments mAbs and IgGs into its $F(ab')_2$ and Fc subunits by cleaving the antibody at specific sites below the hinge region. Both expected fragments could be identified by means of the nES-DMA with SXR (in terms of macromolecule size and MW) and corroborated by MW values obtained by means of MS. Especially working with complex mixtures, the nES-DMA inherent charge-reduction to single charged species allows a simplified data interpretation omitting data deconvolution.

Furthermore, the performance of the instrument analyzing a rmAb was studied with special focus on repeatability and accuracy. Particularly, the size-determination revealed very low variability for both,

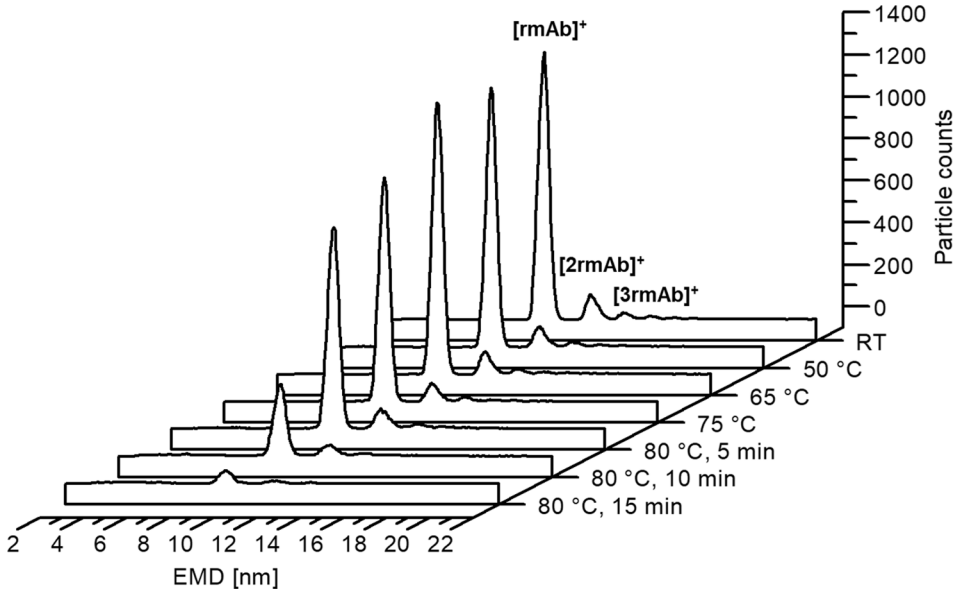

Fig. 7. Nano ES-DMA/SXR analysis of rmAb after incubation at ambient temperature (RT), 50 °C, 65 °C, and 75 °C for 15 min each and at 80 °C for 5, 10, and 15 min.

inter- and intra-day measurements. Moreover, obtained EMDs and correlating MW values were in good agreement to MS results.

In contrast, quantitation showed a higher dependence on measurements performed in one setup or on consecutive days. High standard deviations were found for inter-day experiments, whereas they dropped to a sixth when analyses were carried out during one day runs. Thus, reproducible measurement setups applying well-defined parameters such as the same capillary with excellent tip geometry and the formation of a stable cone-jet mode are of importance. Clouet-Foraison and colleagues found similar effects upon quantification of lipoprotein particles with a modified nES-DMA setup [7].

Replacing the syringe pump for direct infusion with a flow injection analysis (FIA) system or nano HPLC system can further reduce variability and standard deviations. In this regard, the influence of different scan times was investigated. The shorter scan time of 11 s was chosen for fast analysis times needed to detect peaks eluting from a HPLC system optimized for large glycoproteins. The reduction of scan speed induced a slight shift of EMDs to higher values. However, deviations in the calculation of the rmAb MW are compensated, as the lower scan time also influences the EMDs of the standards used for the EMD/MW correlation. Next to that, scan times significantly affected signal intensities. With lower peak heights but at the same time broader peaks, resolution declines with a scan time of 11 s. Thus, longer scan times of 56 s with higher resolving powers in terms of sizing and sensitivity were favorable measurement parameters for direct infusion. In case of on-line coupling with nano HPLC a balance between optimal resolving power of the DMA and scan time of the DMA (i.e. fitting to the peak width of the chromatographic peak) has to be found.

Besides characterizing the rmAb in respect to its size, oligomers/aggregation, or degradation, a variation of pH and temperature can be induced in order to simulate forced stress conditions. The reduction of pH from 8.0 to 5.0 did not show any influence on the particular rmAb itself. Except from overall higher peak areas and widths, no degradation products or shifts in EMD values were observable. Additionally, multimer formation was not affected as the relative ratios of dimers and trimers in regard to the monomer did not alter significantly: 10 % dimers and 3 % trimers at pH 8.0 and 12 % dimers and 4 % trimers at pH 5.0 were detected.

Also, incubations of the rmAb up to 70 °C did not impact results as indicated by a comparable signal over stressing along several temperatures. However, a decrease of the rmAb signal was observed after incubations above 75 °C. As no soluble degradation or aggregation products were detected (and nES-DMA with SXR is in principle capable to do so as demonstrated), sample loss due to sedimentation and adsorption at the inner wall of the reaction tube during incubation was concluded.

5. Conclusion

In summary, nES-DMA with SXR proved to be a suitable tool for recombinant monoclonal antibody analysis and the investigation of its purity, quality, and stability during quality control, monitoring of production processes or stress studies. The system clearly demonstrated its ability to in principle perform separations of oligomers/aggregates as well as large fragments next to intact rmAb in gas-phase under atmospheric pressure. In this context sample analysis at different analyte concentrations enables the differentiation of biospecific and nES induced aggregation. nES-DMA with SXR further allows for highly reproducible and accurate size determinations at high sensitivity rendering it a valuable device for biotechnological applications.

CRediT authorship contribution statement

Nicole Y. Engel: Formal analysis, Writing – original draft. **Nicole Puffler:** Formal analysis. **Martina Marchetti-Deschmann:** Supervision, Writing – review & editing. **Günter Allmaier:** Conceptualization, Funding acquisition, Resources, Supervision, Writing – review & editing. **Victor U. Weiss:** Supervision, Project administration, Data curation, Writing – review & editing.

Declaration of Competing Interest

The authors declare that they have no known competing financial interests or personal relationships that could have appeared to influence the work reported in this paper.

Acknowledgement

This project was funded partly by the Austrian Science Foundation (FWF, Project Number TRP 29-N20). The authors acknowledge TU Wien Bibliothek for financial support through its Open Access Funding Programme.

Appendix A. Supplementary data

Supplementary data to this article can be found online at https://doi.org/10.1016/j.jchromb.2021.122925.

References

[1] C. Cruz-Teran, K. Tiruthani, M. McSweeney, A. Ma, R. Pickles, S.K. Lai, Challenges and opportunities for antiviral monoclonal antibodies as COVID-19 therapy, Adv. Drug Deliv. Rev. 169 (2021) 100–117, https://doi.org/10.1016/j.addr.2020.12.004.

[2] J.Z. Bereszczak, M. Havlik, V.U. Weiss, M. Marchetti-Deschmann, E. van Duijn, N. R. Watts, P.T. Wingfield, G. Allmaier, A.C. Steven, A.J. Heck, Sizing up large protein complexes by electrospray ionisation-based electrophoretic mobility and native mass spectrometry: morphology selective binding of Fabs to hepatitis B virus capsids, Anal. Bioanal. Chem. 406 (2014) 1437–1446, https://doi.org/10.1007/s00216-013-7548-z.

[3] N.Y. Engel, V.U. Weiss, M. Marchetti-Deschmann, G. Allmaier, nES GEMMA Analysis of Lectins and Their Interactions with Glycoproteins - Separation, Detection, and Sampling of Noncovalent Biospecific Complexes, J. Am. Soc. Mass. Spectrom. 28 (2017) 77–86, https://doi.org/10.1007/s13361-016-1483-0.

[4] S.L. Kaufman, J.W. Skogen, F.D. Dorman, F. Zarrin, K.C. Lewis, Macromolecule analysis based on electrophoretic mobility in air: globular proteins, Anal. Chem. 68 (1996) 1895–1904, https://doi.org/10.1021/ac951128f.

[5] J.F. de la Mora, L. de Juan, T. Eichler, J. Rosell, Differential mobility analysis of molecular ions and nanometer particles, Trends Anal. Chem. 17 (1998) 328–339, https://doi.org/10.1016/S0165-9936(98)00039-9.

[6] S.L. Kaufman, Analysis of biomolecules using electrospray and nanoparticle methods: the gas-phase electrophoretic mobility molecular analyzer (GEMMA), J. Aerosol Sci. 29 (1998) 537–552, https://doi.org/10.1016/S0021-8502(97)00462-X.

[7] N. Clouet-Foraison, F. Gaie-Levrel, L. Coquelin, G. Ebrard, P. Gillery, V. Delatour, Absolute Quantification of Bionanoparticles by Electrospray Differential Mobility Analysis: An Application to Lipoprotein Particle Concentration Measurements, Anal. Chem. 89 (2017) 2242–2249, https://doi.org/10.1021/acs.analchem.6b02909.

[8] S. Mouradian, J.W. Skogen, F.D. Dorman, F. Zarrin, S.L. Kaufman, L.M. Smith, DNA analysis using an electrospray scanning mobility particle sizer, Anal. Chem. 69 (1997) 919–925, https://doi.org/10.1021/ac960785k.

[9] C.S. Kaddis, J.A. Loo, Native protein MS and ion mobility: large flying proteins with ESI, Anal. Chem. 79 (2007) 1778–1784, https://doi.org/10.1021/ac071878c.

[10] L.F. Pease 3rd, J.T. Elliott, D.H. Tsai, M.R. Zachariah, M.J. Tarlov, Determination of protein aggregation with differential mobility analysis: application to IgG antibody, Biotechnol. Bioeng. 101 (2008) 1214–1222, https://doi.org/10.1002/bit.22017.

[11] S. Guha, M. Li, M.J. Tarlov, M.R. Zachariah, Electrospray-differential mobility analysis of bionanoparticles, Trends Biotechnol. 30 (2012) 291–300, https://doi.org/10.1016/j.tibtech.2012.02.003.

[12] L.F. Pease 3rd., Physical analysis of virus particles using electrospray differential mobility analysis, Trends Biotechnol. 30 (2012) 216–224, https://doi.org/10.1016/j.tibtech.2011.11.004.

[13] V.U. Weiss, J.Z. Bereszczazk, M. Havlik, P. Kallinger, I. Gosler, M. Kumar, D. Blaas, M. Marchetti-Deschmann, A.J. Heck, W.W. Szymanski, G. Allmaier, Analysis of a common cold virus and its subviral particles by gas-phase electrophoretic mobility molecular analysis and native mass spectrometry, Anal. Chem. 87 (2015) 8709–8717, https://doi.org/10.1021/acs.analchem.5b01450.

[14] V.U. Weiss, R. Pogan, S. Zoratto, K.M. Bond, P. Boulanger, M.F. Jarrold, N. Lyktey, D. Pahl, N. Puffler, M. Schelhaas, E. Selivanovitch, C. Uetrecht, G. Allmaier, Virus-like particle size and molecular weight/mass determination applying gas-phase electrophoresis (native nES GEMMA), Anal. Bioanal. Chem. 411 (2019) 5951–5962, https://doi.org/10.1007/s00216-019-01998-6.

[15] V.U. Weiss, C. Urey, A. Gondikas, M. Golesne, G. Friedbacher, F. von der Kammer, T. Hofmann, R. Andersson, G. Marko-Varga, M. Marchetti-Deschmann, G. Allmaier, Nano electrospray gas-phase electrophoretic mobility molecular analysis (nES GEMMA) of liposomes: applicability of the technique for nano vesicle batch control, Analyst 141 (2016) 6042–6050, https://doi.org/10.1039/c6an00687f.
[16] G. Taylor, Disintegration of water drops in electric field, Proc. R. Soc. Lond. A Math. Phys. Sci. 280 (1964) 383–397, https://doi.org/10.1098/rspa.1964.0151.
[17] M. Cloupeau, B. Prunet-Foch, Electrostatic spraying of liquids in cone-jet mode, J. Electrostat. 22 (1989) 135–159, https://doi.org/10.1016/0304-3886(89)90081-8.
[18] D.-R. Chen, D.Y.H. Pui, S.L. Kaufman, Electrospraying of conducting liquids for monodisperse aerosol generation in the 4 nm to 1.8 μm diameter range, J. Aerosol Sci. 26 (1995) 963–977, https://doi.org/10.1016/0021-8502(95)00027-A.
[19] A. Wiedensohler, An approximation of the bipolar charge distribution for particles in the sub-micron size range, J. Aerosol Sci. 19 (1988) 387–389, https://doi.org/10.1016/0021-8502(88)90278-9.
[20] P. Kallinger, W.W. Szymanski, Experimental determination of the steady-state charging probabilities and particle size conservation in non-radioactive and radioactive bipolar aerosol chargers in the size range of 5–40 nm, J. Nanopart. Res. 17 (2015) 171, https://doi.org/10.1007/s11051-015-2981-x.
[21] G. Allmaier, V.U. Weiss, N.Y. Engel, M. Marchetti-Deschmann, W.W. Szymanski, Soft X-ray Radiation Applied in the Analysis of Intact Viruses and Antibodies by Means of Nano Electrospray Differential Mobility Analysis In: Molecular Technologies for Detection of Chemical and Biological Agents, J.H. Banoub, R.M. Caprioli (Eds.) Springer Netherlands: Dordrecht (2017) 149–157, https://doi.org/10.1007/978-94-024-1113-3_9.
[22] V.U. Weiss, J. Frank, K. Piplits, W.W. Szymanski, G. Allmaier, Bipolar Corona Discharge-Based Charge Equilibration for Nano Electrospray Gas-Phase Electrophoretic Mobility Molecular Analysis of Bio- and Polymer Nanoparticles, Anal. Chem. 92 (2020) 8665–8669, https://doi.org/10.1021/acs.analchem.0c01904.
[23] K.C. Lewis, D.M. Dohmeier, J.W. Jorgenson, S.L. Kaufman, F. Zarrin, F.D. Dorman, Electrospray-condensation particle counter: a molecule-counting LC detector for macromolecules, Anal. Chem. 66 (1994) 2285–2292, https://doi.org/10.1021/ac00086a014.
[24] G.J. Sem, Design and performance characteristics of three continuous-flow condensation particle counters: a summary, Atmos. Res. 62 (2002) 267–294, https://doi.org/10.1016/S0169-8095(02)00014-5.
[25] G. Bacher, W.W. Szymanski, S.L. Kaufman, P. Zollner, D. Blaas, G. Allmaier, Charge-reduced nano electrospray ionization combined with differential mobility analysis of peptides, proteins, glycoproteins, noncovalent protein complexes and viruses, J. Mass Spectrom. 36 (2001) 1038–1052, https://doi.org/10.1002/jms.208.
[26] V.U. Weiss, N. Denderz, G. Allmaier, M. Marchetti-Deschmann. Online hyphenation of size-exclusion chromatography and gas-phase electrophoresis facilitates the characterization of protein aggregates. Electrophoresis. (2021) Epub ahead of print. https://doi.org/10.1002/elps.202100018.
[27] M. Li, S. Guha, R. Zangmeister, M.J. Tarlov, M.R. Zachariah, Quantification and compensation of nonspecific analyte aggregation in electrospray sampling, Aerosol Sci. Technol. 45 (2011) 849–860, https://doi.org/10.1080/02786826.2011.566901.